Case Studies in Thermal Engineering 42 (2023) 102707

Contents lists available at ScienceDirect

Case Studies in Thermal Engineering

journal homepage: www.elsevier.com/locate/csite

Numerical Crank-Nicolson methodology analysis for hybridity aluminium alloy nanofluid flowing based-water via stretchable horizontal plate with thermal resistive effect

Hanifa Hanif [a,b], Wasim Jamshed [c,*], Mohamed R. Eid [d,e], Suriya Uma Devi S [f], Rabha W. Ibrahim [g], Sharidan Shafie [b], Aeshah A. Raezah [h], Sayed M. El Din [i]

[a] Department of Mathematics, Sardar Bahadur Khan Women's University, Quetta, Pakistan
[b] Department of Mathematical Sciences, Faculty of Science, Universiti Teknologi Malaysia, 81310, Johor Bahru, Johor, Malaysia
[c] Department of Mathematics, Capital University of Science and Technology (CUST), Islamabad, 44000, Pakistan
[d] Department of Mathematics, Faculty of Science, New Valley University, Al-Kharga, Al-Wadi Al-Gadid, 72511, Egypt
[e] Department of Mathematics, Faculty of Science, Northern Border University, Arar, 1321, Saudi Arabia
[f] Department of Mathematics, KPR Institute of Engineering and Technology, Coimbatore, 641407, India
[g] Department of Computer Science and Mathematics, Lebanese American University, 13-5053, Beirut, Lebanon
[h] Department of Mathematics, Faculty of Science, King Khalid University, Abha, 62529, Saudi Arabia
[i] Center of Research, Faculty of Engineering, Future University in Egypt New Cairo 11835, Egypt

ARTICLE INFO

Handling Editor: Huihe Qiu

Keywords:
Hybrid nanofluid
Magnetohydrodynamics
Joule heating
Crank-Nicolson method

ABSTRACT

Hybrid nanofluid (HNF) is a new and improved type of nanofluid models that is widely employed in fluid flow regimes to increase thermal efficiency. The purpose of this effort is to investigate HNF flow in two dimensions over a horizontal sheet while accounting for the effects of Joule heating, viscous dissipation, suction, and thermal slip. The impact of regulating parameters on skin friction and heat transfer is also investigated. HNF used in this investigation is a mixture of water and two types of solid nanoparticles, namely aluminium alloys AA7072 and AA7075. The numerical solutions of partial differential equations are obtained using the Crank-Nicolson method. The outcomes are illustrated in detailed ranges of the connection parameters. The thermal slip effect diminishes the temperature outline from the system and wall temperature. Shrinking sheet movement plays a key role in manipulating fluidity and thermal dispersal. Magnetic strength pulls down the fluidity and wall temperature meanwhile, it assists the thermal dispersion, fractional force, and Nusselt number.

1. Introduction

Nanofluids are two-phase liquid-solid combination fluids that may be thought of as next-generation heat-transference fluids. Nanofluids have a bright future as thermal fluids in a variety of heat transference implementations. Since solid nanomaterials with characteristic length scales of 1–100nm and high current conductivity are adjourned in the base fluid, they have improved the conventional fluid's effective thermal conducting and convection heat transference. There are improved conceptions and actual uses of nanofluids that provide exciting heat transference features when compared to traditional heat transference fluids, such as solar cells, electrical substation implementations, and cooling systems [1,2].

* Corresponding author.
E-mail address: wasiktk@hotmail.com (W. Jamshed).

https://doi.org/10.1016/j.csite.2023.102707
Received 1 November 2022; Received in revised form 2 January 2023; Accepted 4 January 2023
Available online 5 January 2023

Nanofluid models are extremely important to scientists since they have substantial manufacturing and engineering applications due to their increased heat transfer rates. HNF is a term used to describe a homogenous phase created by mixing two or more metals at the same time. When compared to unitary NF, this progressive class of HNF showed promising improvements in heat transfer properties, thermo-physical and hydrodynamic properties. HNF can be engaged in a variety of heat transfer (HT) applications, involving transportation, engineering, and health sciences. Deferment of various nanofluid models in a composite/mixture of base fluids can be used to make HNF. HT system is critical in many sectors involving thermal and chemical processes. Fluids are constantly used in HT process. The major goal of using mixes (HNF) is to increase the efficacy of the mixture's thermal characteristics, and hybridity nanofluid is a mixing of different nano-sized particles with fluid. Numerous strategies have been used in reality to improve the thermal characteristics of liquids. In terms of boosting HT efficiency, nanoparticles are the most prevalent and up-to-date technical trend. In the presence of rotation, Said et al. [3] proposed a 3D class of HNF to further increase the HT rate over the stretching sheet. Mandal et al. [4] utilized an artificial neural network to shape investigational data. Saha et al. [5] reported a study of HT and rheological properties of HNFs for cooling applications. The findings of this investigation would be useful to the developer in helping them model the thermal device while taking numerous regulating factors into proper thermal management. Review investigation by Al-Chlaihawi et al. [6] probed the heat convection, fluid flow, and entropy formation in porousness enclosures filled with hybridity nanofluid is summarized in this work. The effects of magnetohydrodynamics on Newtonianism and non-Newtonianism base fluids are studied. Natural convective HT is one of the most prevalent kinds of HT due to the vast range of technical implications it has, including solar panels, electronic devices, air conditioners, nuclear reactors, and geothermal operational. Tayebi [7] analysed local non-equilibria on the natural convective heat transfer in a non-Darcy porous medium. Tayebi et al. [8] analysed local non-equilibrium over a saturated horizontal elliptical non-Darcian porous annulus. Kursus et al. [9] discussed the most current advancements in nanofluids and hybridity nanofluids in machining operations such as milling, turning, grinding, and drilling nanofluid and HNF thermophysical qualities such as viscidness, heat conductance, durability, and hydrophilicity Thermal conductivity and viscosity of nanofluids were shown to be highly impacted by temperature, mass fractional size, particles kind, and nanomolecules size. HNF has better thermophysical characteristics than nanofluids and conventional fluids. Xiong et al. [10] examined the recent studies in this field to determine the primary benefits and drawbacks of HNF as HT agents in solar energy collectors. Muneeshwaran et al. [11] presented a state-of-the-art overview on the use of HNF in diverse heat transfer applications, as well as the limitations associated with HNF and future research directions. While Dubey et al. [12] presented a short review in HNF on mechanics studies. These review examinations offered a set of connections between thermophysical characteristics. For several heat transference applications, the relationships between the Nusselt quantity and frictional factor are also listed. Finally, the difficulties with mono nanofluids, hybridity nanofluids, and potential future study areas are discussed. Syed and Jamshed [13] looked at the flow of MHD tangent HNF over a stretched sheet's boundary layer. In addition, the application of the generalized HT of tangent hyperbolic fluids across a nonlinearly ranging slip including HNFs was examined by Refs. [14–16].

A magnetic field (MF) in a fluid is a field of force produced by a magnet or by an electric current flowing through the fluid. It is similar to a magnetic field in a vacuum, but the properties of the fluid can affect the strength and distribution of the field. For example, the presence of ferromagnetic materials in the fluid can increase the field strength (Zhang et al. [17] and Hanif et al. [18,19]), and the fluid's electrical conductivity can affect the field's distribution (Mourad et al. [20] and Manna et al. [21]). The magnetic field in a fluid can be used for a variety of purposes, such as magnetic resonance imaging (MRI) in medicine and magnetohydrodynamic (MHD) propulsion in aerospace (Khashi'ie et al. [22]). It can also be used to study the properties of the nanofluid itself, as the field can interact with the nanoparticles and provide information about their size, shape, and concentration (Saqib et al. [23], Hanif et al. [24], and Alkasasbeh et al. [25]). Different studies and computational analysis are done by Roy et al. [26]. While, and Khazayinejad and Nourazar [27] considered the concept of fractional calculus to designate HT investigation of HNF along a leaky platter. Gürdal et al. [28] impacted the HNF flowing in an indented tube endangered with the MF. In the manifestation of Joule heating, the magnetic flowing and HT of HNF passes a diminishing cylinder are elaborated by Khashi'ie et al. [29]. HT rate is reduced by both the Eckert quantity and the curvature variable. The curvature variable, on the other hand, enhances boundary layer separation, but an increase in Eckert quantity has no impact on slowing boundary layer separation. Shoaib et al. [30] explored the phenomena of HT in 3D radiative flowing of HNF via a spinning disc using magnetic force and Joule heating. The rate of HT is shown to be related to the Brinkman quantity, electromagnetic impact, and nanomolecules concentricity. Hanifa and Shafie [31,32] probed the magneto effect on HNF flowing with HT over a horizontal flat surface, correspondingly, with MF. The radiation and magneto micropolar HNF flowing via a stretchable (shrinkable) sheet of Al_2O_3 and Cu nanostructures is investigated by Waini et al. [33]. Furthermore, the effects of Joule heating and viscid dissipative flow are considered. The impact of Eckert quantity and Thermal radiation variable on HT rate is to diminish it. Zainal et al. [34] quantitatively investigated the conduct of magnetic effect on the unsteadiness separate stagnating-point flowing of HNF with the effects of viscid dissipative flow and Joule heating. Recent developments in the hybrid nanofluid research can be found in Ref. [35to39].

The Crank-Nicolson method can be used to solve time-dependent partial differential equations (PDEs) that describe fluid flow. For example, the Navier-Stokes equations are a set of PDEs that describe the motion of viscous fluid and are commonly used to model fluid flow. The Crank-Nicolson method can be used to solve the Navier-Stokes equations in two dimensions (e.g., for a flat surface) by breaking the surface into a grid of discrete points and approximating the derivatives in the equations using finite differences. The resulting system of equations can then be solved iteratively using the Crank-Nicolson method. One advantage of using the Crank-Nicolson method to solve the Navier-Stokes equations is that it is unconditionally stable, meaning that it is stable for any choice of time step size. This is in contrast to explicit methods, which can become unstable if the time step size is too large. It is worth noting that solving the Navier-Stokes equations is a challenging task, and it is not always possible to obtain an analytical solution. In these cases, numerical methods such as the Crank-Nicolson method can be used to approximate the solution [40]. In terms of time, it is a 2nd-order technique. It is numerically stable, implicit in time, and may be stated as an implicit Runge-Kutta technique [41]. To investigate the supercritical behaviour of 3rd-grid aqueous nanofluid in perspective of supercritical water, a novel computational thermodynamic model is presented by Hiremath et al. [42]. The Redlich-Kwong formula of state was used to compute the thermal expansion rate for supersonic nanofluid free convection in terms of temperature, compaction factor, and pressure. To get numerical solutions, a well-tested unconditionally stable Crank-Nicolson technique was used. Hanif [43,44] explored the heat transference and unsteadiness flowing features of a Maxwell fluid over a vertical flat surface. The numerical finite-difference approach in the Crank Nicolson style is used to solve the model of governing boundary layer flowing and heat transmission. In the occurrence of a magneto force and radiative fluxing, a mathematical model is developed by Hiremath et al. [45] to analyse the unsteadiness magneto-convection flowing and heat transition attributes of 3rd-grade Reiner-Rivlin non-Newtonianism nanofluid from a moving or stationary hot cylinder. A well-proven convergent Crank-Nicolson type finite difference technique is employed.

As a consequence of the above-declared investigations, the recent exploration aims are to consider the 2D-magnetohydrodynamics AA7072+AA7075 HNF crossways a perpendicular rabidly decrease slip by the reality of Joule heating and thermal slide condition. The single-phase NFM of Tiwari and Das are employed in this analysis. HNF-containing aluminium alloys (AA7072) and (AA7075) nanoparticles were employed in this study to attain outstanding convective heat transfer efficiency. HNF (AA7072+AA7075/water) is created by suspending two nanoparticles. This research looks at the velocity and temperature profiles of solid nanoparticles with different volume fractions, magnetic properties, Eckert numbers, thermal slip parameters, and Prandtl numbers. This study also investigates the effect of solid copper nanoparticles against suction on variations of reduced skin friction and concentrated heat transfer. The existing numerical findings are associated to the outcomes of earlier investigations for comparison. According to best our understanding, this is the unique and novel attempt to engage the Numerical Crank-Nicolson Methodology to analysing thermal resistive effect using Hybridity Aluminium Alloy Nanofluid Flowing Based-Water via Stretchable Horizontal Plate. Applicability of this problem can be found in the industrial, manufacturing and research laboratories were the metal rods and sheets were treated at high temperatures and requiring cooling process for the finishing effects of the products. Numerical prediction through this work can help the experimenters to optimize their process towards successful outcomes with minimal failure rate.

2. Mathematical formulation

The two-dimensional incompressible, unsteady MHD flow of HNF over a horizontal stretching sheet in the presence of viscous dissipation is stated (Fig. 1S (supplementary material)).

In $x-$ axis manner, the shallow velocity is $u = U_w(x/L)$. Furthermore, the thermal slip condition is implemented at the surface of the sheet. Besides, along $y-$ axis, a MF of strength B_0 is used. The central equation for a HNF is given by the following set of equations

$$\frac{\partial u^*}{\partial x^*}+\frac{\partial u^*}{\partial y^*}=0. \tag{1}$$

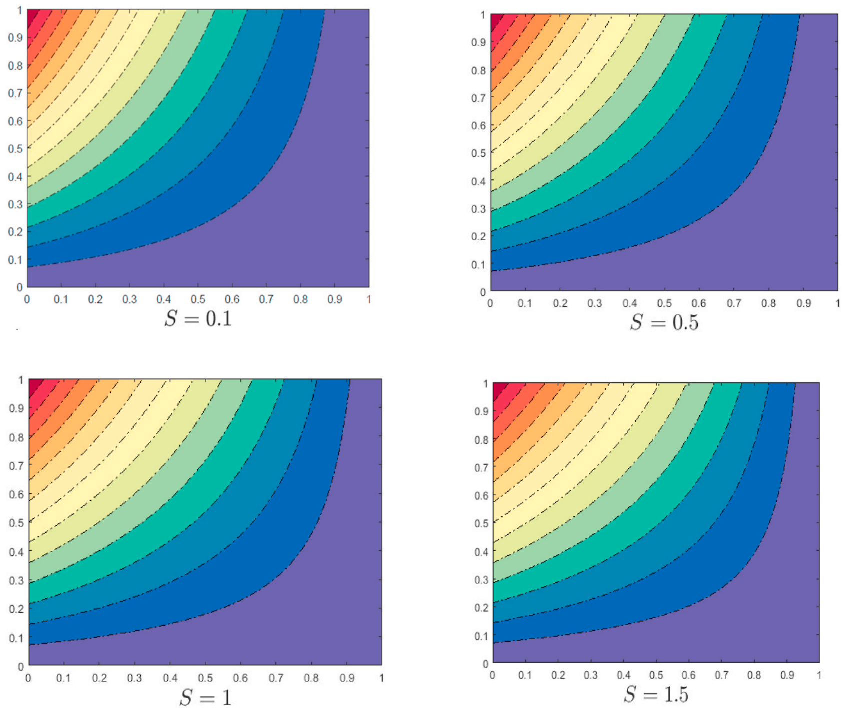

Fig. 1. Velocity contour plots for various values of suction (S).

$$\rho_{hnf}\left(\frac{\partial u^*}{\partial t}+u^*\frac{\partial u^*}{\partial x^*}+v^*\frac{\partial u^*}{\partial y^*}\right)=\mu_{hnf}\frac{\partial^2 u^*}{\partial y^{*2}}-\sigma_{hnf}B_0^2u^*. \tag{2}$$

$$(\rho C_p)_{hnf}\left(\frac{\partial T^*}{\partial t}+u^*\frac{\partial T^*}{\partial x^*}+v^*\frac{\partial T^*}{\partial y^*}\right)=k_{hnf}\frac{\partial^2 T^*}{\partial y^{*2}}+\mu_{hnf}\left(\frac{\partial u^*}{\partial y^*}\right)^2+\sigma_{hnf}B_0^2u^{*2}. \tag{3}$$

The corresponding initial boundary conditions are

$$\left.\begin{array}{c} u^*(x^*,y^*,0)=0, v(x^*,y^*,0)=0, T^*(x^*,y^*,0)=0,\\ u^*(0,y^*,t)=0, T^*(0,y^*,t)=T_\infty,\\ u^*(x^*,0,t)=U_w\left(\frac{x}{L}\right), v^*(x^*,0,t)=V_w, T^*(x^*,0,t)=T_w+\beta\frac{\partial T^*}{\partial y^*},\\ u^*(x^*,\infty,t)=0, T^*(x^*,\infty,t)=T_\infty. \end{array}\right\} \tag{4}$$

The velocity constituents u^* and v^* along with the x^*- axis, and y^*- axis are suggested correspondingly. Though, β is the aspect of thermal slip, while T denotes the temperature. HNF thermo physical possessions were utilized to control the overhead equation, as declared in Table 1 and Table 2. Solid nanoparticles volume fractions of aluminum alloys AA7072 and AA7075is articulated by φ_1 and φ_2 singly. Additionally, $C_p, \mu, \rho, \sigma,$ and k denote the detailed temperature capability, dynamic viscidness, thickness, electrical conductivity, and thermal conductivity, respectively. The subscripts f, nf, hnf, s_1 and s_2 represent fluid, NF, HNF, solid nanoparticles 1 (AA7072), and solid nanoparticles 2 (AA7075), correspondingly.

Introducing an appropriate set of non-dimensional parameters

$$x=\frac{x^*}{L}, y=y^*\left(\frac{U_w}{\nu_f L}\right)^{\frac{1}{2}}, t=\frac{U_w t^*}{L}, u=\frac{uu^*}{U_w}, v=v^*\left(\frac{U_w\nu_f}{L}\right)^{\frac{-1}{2}}, T=\frac{T^*-T_\infty}{T_w-T_\infty}, \tag{5}$$

The non-dimensional form of equations (2), (3) and (6) are [46].

$$\frac{\partial u}{\partial x}+\frac{\partial v}{\partial y}=0, \tag{6}$$

$$\frac{\rho_{hnf}}{\rho_f}\left(\frac{\partial u}{\partial t}+u\frac{\partial u}{\partial x}+v\frac{\partial u}{\partial y}\right)=\frac{\mu_{hnf}}{\mu_f}\frac{\partial u^2}{\partial y^2}-\frac{\sigma_{hnf}}{\sigma_f}Mu, \tag{7}$$

$$\frac{(\rho C_p)_{hnf}}{(\rho C_p)_f}\left(\frac{\partial T}{\partial t}+u\frac{\partial T}{\partial x}+v\frac{\partial T}{\partial y}\right)=\frac{k_{hnf}}{k_f\,Pr}\frac{\partial^2 T}{\partial y^2}+\frac{\mu_{hnf}Ec}{\mu_f}\left(\frac{\partial u}{\partial y}\right)^2+\frac{\sigma_{hnf}}{\sigma_f}MEcu^2. \tag{8}$$

The non-dimensional initial boundary conditions are

$$\left.\begin{array}{c} u(x,y,0)=0, v(x,y,0)=0, T(x,y,0)=0,\\ u(0,y,t)=0, T(0,y,t)=0,\\ u(x,0,t)=x, v(x,0,t)=S, T(x,0,t)=1+\gamma\frac{\partial T}{\partial y},\\ u(x,\infty,t)=0, T(x,\infty,t)=T_\infty. \end{array}\right\} \tag{9}$$

Table 1
HNF thermophysical physiognomies [47].

Titles	Appearances
Dynamic Viscosity	$\mu_{hnf}=\frac{\mu_f}{(1-\varphi_1)^{2.5}(1-\varphi_2)^{2.5}}$
Electrical conductivity	$\sigma_{hnf}=\frac{\sigma_2+2\sigma_{nf}-2\varphi_2(\sigma_{nf}-\sigma_2)}{\sigma_2+2\sigma_{nf}+\varphi_2(\sigma_{nf}-\sigma_2)}\times(\sigma_{nf})$
	where $(\sigma_{nf})=\frac{\sigma_1+2\sigma_f-2\varphi_1(\sigma_f-\sigma_1)}{\sigma_1+2\sigma_f+\varphi_1(\sigma_f-\sigma_1)}\times(\sigma_f)$
Thermal conductivity	$k_{hnf}=\frac{k_{s2}+2k_{nf}-2\varphi_2(k_{nf}-k_{s2})}{k_{s2}+2k_{nf}+\varphi_2(k_{nf}-k_{s2})}\times(k_{nf})$
	where $k_{nf}=\frac{k_{s1}+2k_f-2\varphi_1(k_f-k_{s1})}{k_{s1}+2k_f+\varphi_1(k_f-k_{s1})}\times(k_f)$
Heat capacity	$(\rho c_p)_{hnf}=(1-\varphi_2)[(1-\varphi_1)(\rho c_p)_f+\varphi_1(\rho c_p)_{s1}]+\varphi_2(\rho c_p)_{s2}$
Density	$\rho_{hnf}=(1-\varphi_2)[(1-\varphi_1)\rho_f+\varphi_1\rho_{s1}]+\varphi_2\rho_{s2}$

Table 2
Thermal-physical characteristics of solid nanoparticles and base fluid [48].

Fluids	$\rho\ (kg/m^3)$	$\sigma(S/m)$	$c_p(J/kg\,K)$	$k\ (W/m\,K)$	Pr
Water (H_2O)	997.1	0.05	4179	0.613	6.2
AA7072	2810	26.77×10^6	960	173	–
AA7075	2720	34.83×10^6	893	222	–

Here $M = \frac{\sigma_f B_0^2 L}{\rho_f U_w}, Pr = \frac{(\mu C_p)_f}{k_f}, Ec = \frac{U_w^2}{C_p(T-T_\infty)}, S = V_w\left(\frac{L}{U_w \nu_f}\right)^{\frac{1}{2}}$ and $\gamma = \beta\left(\frac{U_w}{\nu_f L}\right)^{\frac{1}{2}}$ are magnetic parameter, Prandtl number, Eckert number, suction parameter, and thermal slip parameter, respectively. The skin friction and Nusselt number are specified as

$$C_f = \frac{\tau_w}{\rho_f U_w^2}, Nu = \frac{x^* q_w}{k_f(T_w - T_\infty)}. \tag{10}$$

where $\tau_w = \mu_{hnf}\left(\frac{\partial u}{\partial y}\right)_{y=0}$ and $q_w = -k_{hnf}\left(\frac{\partial T}{\partial y}\right)_{y=0}$. Using the non-dimensional parameters (5), the following non-dimensional form of equation (10) is obtained

$$Nu_x Re^{-1/2} = -\frac{k_{hnf} x}{k_f}\left(\frac{\partial T}{\partial y}\right)_{y=0}, C_f Re^{1/2} = \frac{\mu_{hnf}}{\mu_f}\left(\frac{\partial u}{\partial y}\right)_{y=0}. \tag{11}$$

3. Finite difference method and numerical validity

The Crank-Nicolson method, which approximates the equations at an average of current and forward time levels, i.e., n^{th} and $(n+1)^{th}$ time level is used to approximate the derivative terms in equations (6)–(8). Let $u_{i,j}^n$, $v_{i,j}^n$ and $T_{i,j}^n$ be the numerical approximation of $u(x,y,t)$, $v(x,y,t)$, and $T(x,y,t)$ at time n for any point (x_i, y_j)

$$\frac{u_{i,j-1}^{n+1} - u_{i-1,j-1}^{n+1} + u_{i,j}^{n+1} - u_{i-1,j}^{n+1} + u_{i,j-1}^{n} - u_{i-1,j-1}^{n} + u_{i,j}^{n} - u_{i-1,j}^{n}}{4\Delta x} + \frac{v_{i,j}^{n+1} - v_{i,j-1}^{n+1} + v_{i,j}^{n} - v_{i,j-1}^{n}}{2\Delta y} = 0, \tag{12}$$

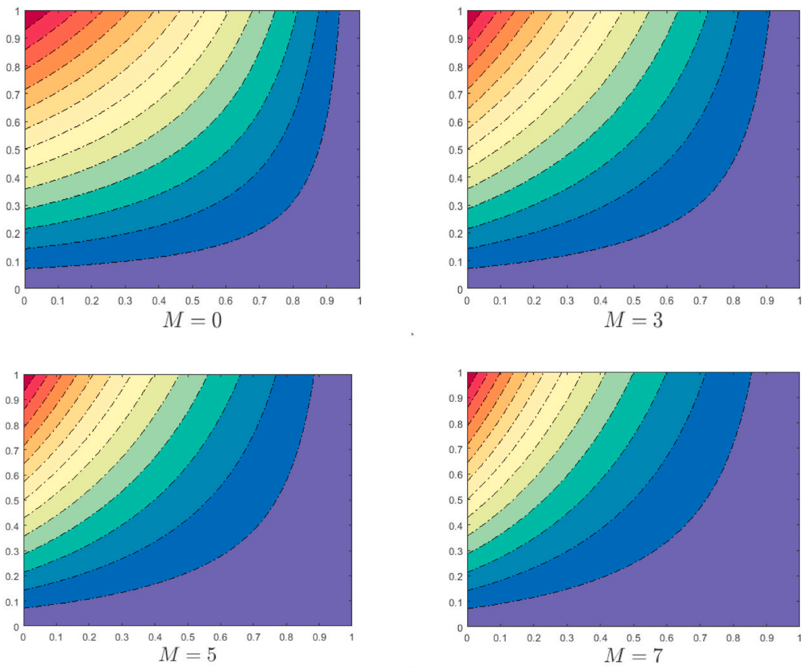

Fig. 2. Velocity contour plots for various values of Magnetic constraints (M).

$$\frac{\rho_{hnf}}{\rho_f}\left(\frac{u_{i,j}^{n+1}-u_{i,j}^{n}}{\Delta t}+u_{i,j}^{n}\frac{u_{i,j}^{n+1}-u_{i-1,j}^{n+1}+u_{i,j}^{n}-u_{i-1,j}^{n}}{2\Delta x}+v_{i,j}^{n}\frac{u_{i,j+1}^{n+1}-u_{i,j-1}^{n+1}+u_{i,j+1}^{n}-u_{i,j-1}^{n}}{4\Delta y}\right)=\frac{\mu_{hnf}}{\mu_f}\left(\frac{u_{i,j+1}^{n+1}-2u_{i,j}^{n+1}+u_{i,j-1}^{n+1}+u_{i,j+1}^{n}-2u_{i,j}^{n}+u_{i,j-1}^{n}}{2\Delta y^2}\right)-M\frac{\sigma_{hnf}}{\sigma_f}\left(\frac{u_{i,j}^{n+1}+u_{i,j}^{n}}{2}\right), \tag{13}$$

$$\frac{(\rho C_p)_{hnf}}{(\rho C_p)_f}\left(\frac{T_{i,j}^{n+1}-T_{i,j}^{n}}{\Delta t}+u_{i,j}^{n}\frac{T_{i,j}^{n+1}-T_{i-1,j}^{n+1}+T_{i,j}^{n}-T_{i-1,j}^{n}}{2\Delta x}+v_{i,j}^{n}\frac{T_{i,j+1}^{n+1}-T_{i,j-1}^{n+1}+T_{i,j+1}^{n}-T_{i,j-1}^{n}}{4\Delta y}\right)=\frac{k_{hnf}}{k_k Pr}\left(\frac{T_{i,j+1}^{n+1}-2T_{i,j}^{n+1}+T_{i,j-1}^{n+1}+T_{i,j+1}^{n}-2T_{i,j}^{n}+T_{i,j-1}^{n}}{2\Delta y^2}\right)+MEc\frac{\sigma_{hnf}}{\sigma_f}\left(\frac{u_{i,j}^{2(n+1)}+u_{i,j}^{2n}}{2}\right)+Ec\frac{\mu_{hnf}}{2\mu_f}\left\{\left(\frac{u_{i,j+1}^{n+1}-u_{i,j}^{n+1}}{\Delta y}\right)^2+\left(\frac{u_{i,j+1}^{n}-u_{i,j}^{n}}{\Delta y}\right)^2\right\}. \tag{14}$$

The mesh size $(\Delta x,\Delta y)=(0.02,0.02)$ in (x,y) direction and time level $(\Delta t=0.01)$ have been used to get the numerical solution. The numerical iterations are performed numerous times to reach the convergent solutions, which are thought to be obtained when the absolute error for all grid nodes approaches $1e^{-5}$.

4. Results and discussions

Fluidity and thermal aspects of the MHD flow of AA7072-AA7075/water over a horizontal sheet subjected to Joule heating and thermal slip condition were studied. Outcomes based on the finite difference exploration such as velocity, temperature, Nusselt number, and surface friction facets were drawn in the form of contour from Figs. 1–6, 1D plots from Figs. 2S-6S (supplementary material), column graphs from Figs. 7 and 8, and through numerical display in Table 3.

The contour plot of velocity for suction effects were portrayed in Fig. 1. For suction ($S > 0$) the flow gets altered to slow down which can be evident through the deep contours away from the wall.

The higher the magnetic interaction more the Lorenz force involves acting against the fluid movement to resist it. Fig. 2 contours clearly depict the above fact with the flocking stream towards the vertical side of the sheet.

Fig. 3 explicates the thermal dispersion in the system of the horizontal stretching sheet. It can be evidently noted through the evenly dispersed isotherms that, for ($S > 0$) suction, along with the shrinking factor, the flow aspects get altered in the way that, it becomes more sensitive around the sheet

Magnetically altered flow rates in the system have worked in favour of thermal transference. For lower values of the magnetic

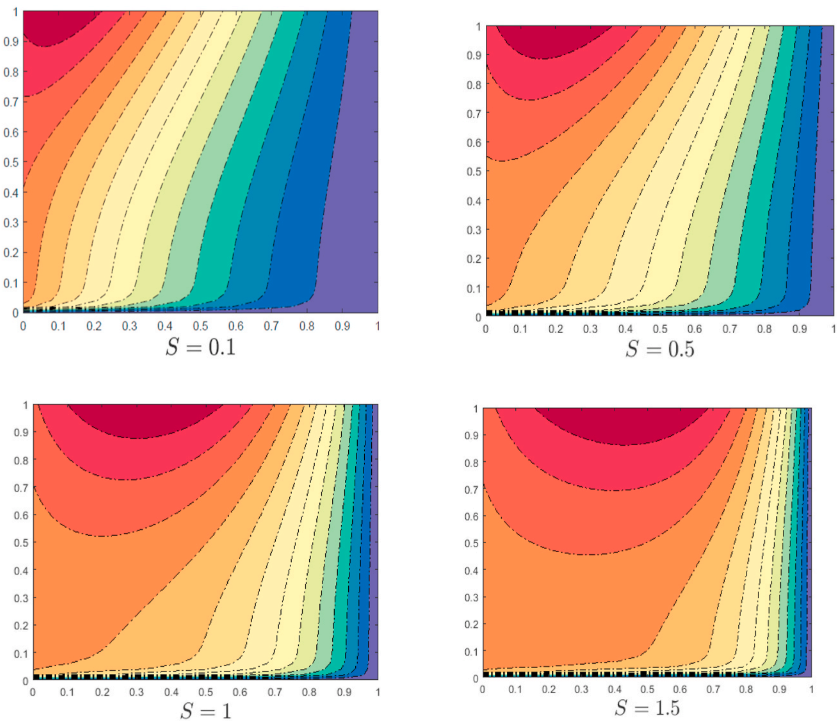

Fig. 3. Temperature contour plots for various values of suction (S).

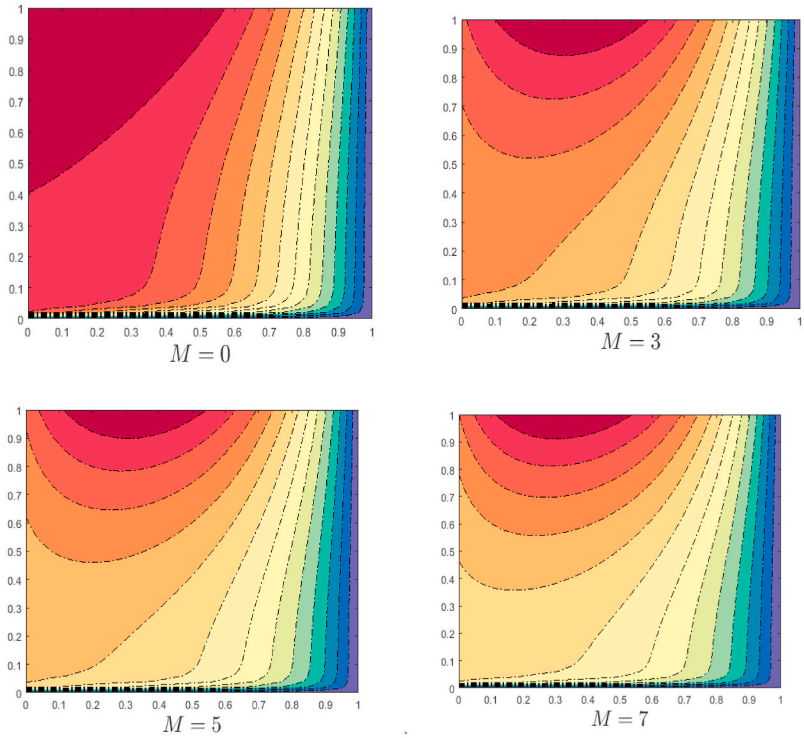

Fig. 4. Temperature contour plots for various values of Magnetic constraints (*M*).

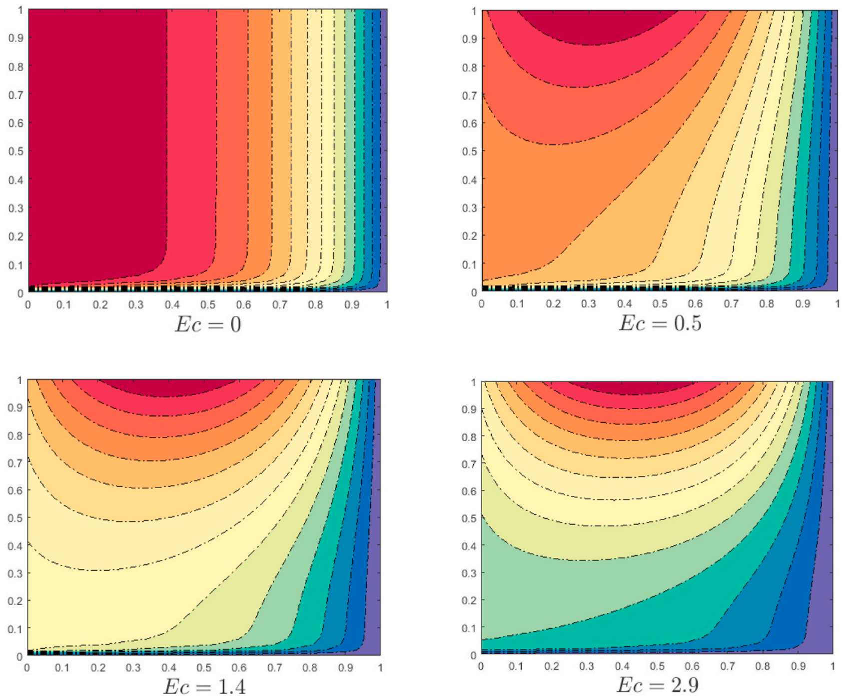

Fig. 5. Temperature contour plots for various values of Eckert number (*Ec*).

constraints (*M*), the denser heat contours were observed adjacent to the sheet. For improving magnetic strength, the temperature around the sheet tends to reduce due to the enhanced thermal transfer with the slower fluid around the sheet which can be noted in Fig. 4 that, moving away from it the significant variation in temperature gets reduced. That is, with the increase in the magnetic force,

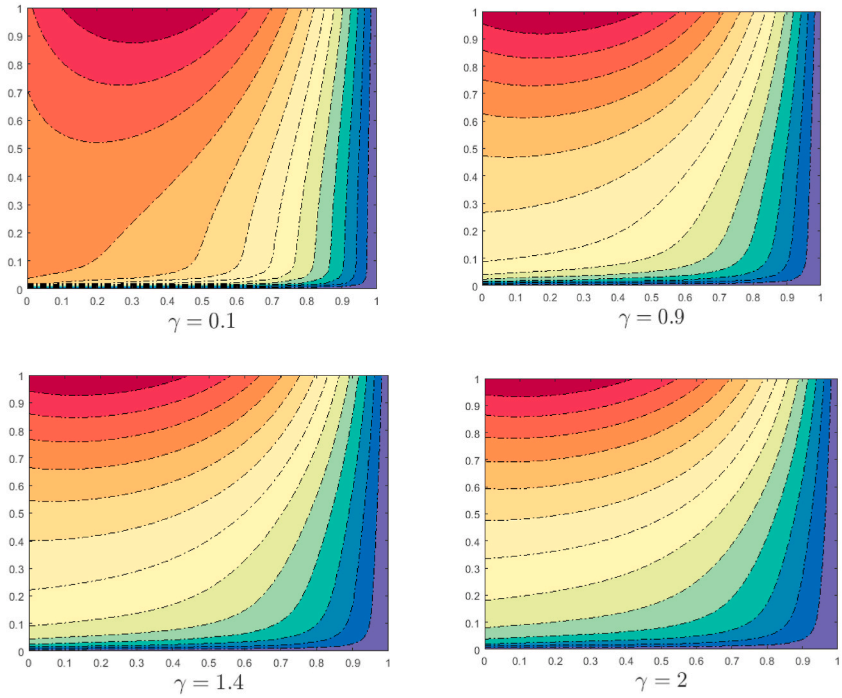

Fig. 6. Temperature contour plots for various values of thermal slip (γ).

the accumulation of temperature outlines boosts away from the boundary layer adjacent to the surface and these outlines crowd away from it. This is physically due to the Lorentz force that dominates with the increase in magnetic force

Eckert number (*Ec*) impacts over the heat dispersal in the system were displayed in Fig. 5. Eckert number reflects the ratio between the mass alterations in the fluid which involve internal friction to the heat dissipation in the system. For initial values of Eckert number (*Ec*), the heat through internal friction seems to be low hence the temperature around the sheet looks dominant. As the Eckert number (*Ec*) grows higher, the heat from internal friction gets significant and the thermal contour gets sifted away from the sheet. Fig. 6 demonstrates the relationship of thermal slippage variable with the temperature outlines. We find that when the value of thermal slippage improves, the value of the temperature enhances as then the outlines begin to approach each other closer to the surface. This shows that the more thermal slippage is reduced, it will contribute to an improvement in the rate of HT. Also, with an increment in the thermal slippage amount, the curvature of the temperature lines boosts towards the upper boundary of the used surface.

Figs. 2S-6S (supplementary material) showcased the physical aspects like flow velocity and temperature dispersal from a one-dimensional point of view. It can be observed that raise in suction tends to boost the flow, meanwhile, the magnetic strength pulls down it.

Through Fig. 2S (supplementary material) , it was found that increasing of the suction values increases the velocity of the fluid flow. While we find that the value of *M* reduces the fluid rapidity as a result of the resistance that the fluid is exposed to from the Lorentz force as shown in Fig. 3S (supplementary material). The raise in the variable of suction enhances the temperature as shown in Fig. 4S (supplementary material). This is because the suction pressure enhances the stored internal energy, which raises the temperature of the fluid. The enhancement of magneto force and Eckert number occurs an increment in the temperature outlines, so we find that there is a clear improvement in temperature with magneto force and Eckert number, as shown in Fig. 5S and 6S (supplementary material). On the other hand, if the thermal dissipation boosts, the temperature is raised a very clear way, while the boost in temperature also occurs with an increment in both the suction amounts and the magnetic force. This is due to the accertion in the energy of the internal particles and the elevetion in the collisions between them, which causes an increase in temperature with the influences mentioned earlier.

4.1. Skin frictional and Nusselt number

To clearly sight the parametrical alterations in the skin frictional and Nusselt number in water, nanofluid (AA7072/water) and hybrid fluid (AA7072- AA7075/water) 3D plots were used in Figs. 7 and 8. Interestingly, because of the shrinkable effect, the frictional impact is greater far a way from the surface than at the near of it which cause the flowing is fasted easily, and it reverses to be slower flowing impacted by existence magnetic strength.

In the suction variations from Fig. 7(a) on the frictional impact, it can be clearly observed that the hybrid combination of fluid attains more frictional impacts than the nanofluid and water. Fig. 7(b) discloses the skin frictional alterations toward the magnetic strength. the frictional importance between the water and nanofluid was higher than that of nanofluid and its hybrid version. As the flow gets slower for higher magnetic influences, the skin resistance tends to be reduced significantly.

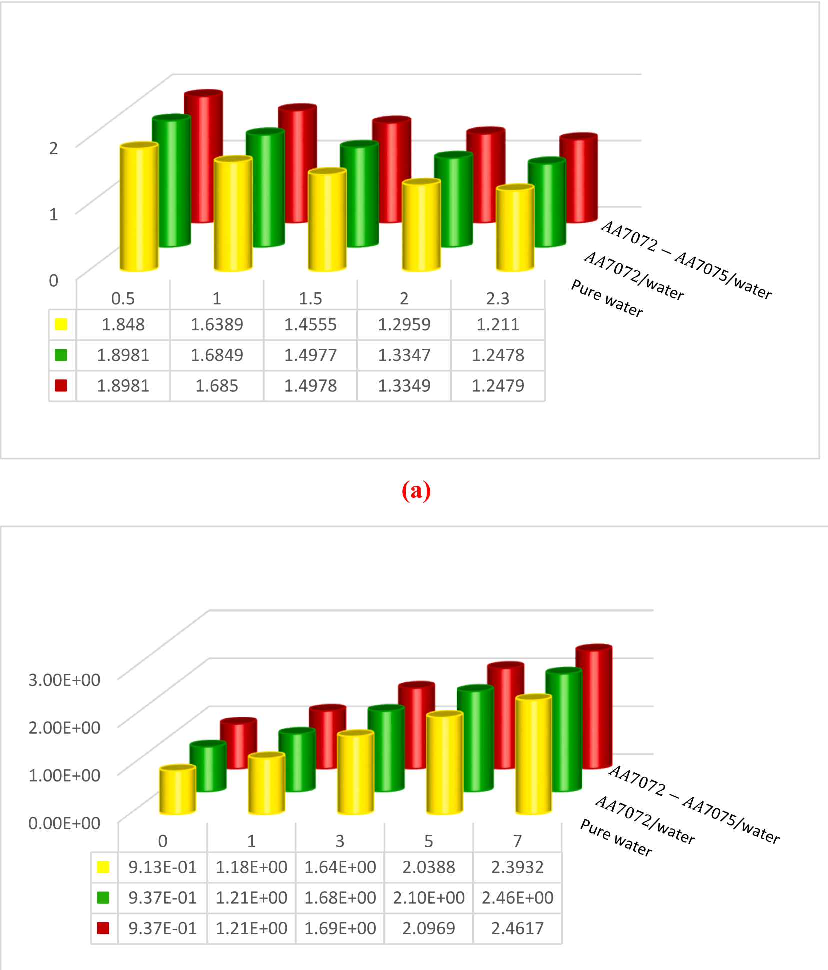

(b)

Fig. 7. Skin friction for various values of (a)Suction (S) and (b) Magnetics constraints (M).

Nusselt number behaviours for parametrical alterations were studied and the results were portrayed in Fig. 8(a–d). Heat transfer in the system can be denoted as the Nusselt number which was studied under the influence of suction, magnetic strength, thermal slip, and Eckert number. Among these, the suction and the thermal slip constraint tend to work against the heat transfer process while the magnetic strength and Eckert number assist the heat transfer and favour the process which can be visualized through the Nusselt number plots. The slow movement of the flowing fluid creates more chances of a thermal transfer process like in the magnetic strength and Eckert number when compared to the suction/injection and thermal slip effects.

Table 3 numerically displays the wall temperature for various parametrical alterations for all three kinds of flow fluids involved in this problem. Change in wall temperature reflects the thermal transfer that occurs due to the parametrical impacts. The trend of numerical values in Table 3 clarifies the fact of engaging hybrid fluids in the palace of traditional nanofluid or pure water. Flow across the sheet for suction values and the thermal slip values reduce the wall temperature. On other hand, a rise in wall temperature happens for increasing values of Magnetic strength and Eckert number.

5. Conclusions

Flow and temperature characteristics of the AA7072+AA7075 Hybrid Nanofluid over a vertical sheet that exponentially shrinks subjected to MHD, Joule heating, and thermal slip conditions were studied. A finite difference scheme is employed to obtain results for velocity, temperature, Nusselt number, and skin friction facets were drawn in the form of plots from Figs. 1–8 and in Table 3. From the result analysis, the following conclusive factors were obtained.

- Suction flow across the sheet tends to elevate the flow velocity, thermal dispersal, and skin frictional aspects.
- Magnetic strength pulls down the fluidity and wall temperature meanwhile, it assists the thermal dispersion, skin fractional, and Nusselt number.

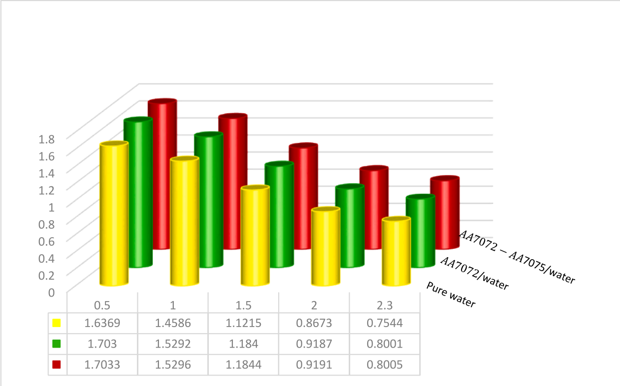

(a)

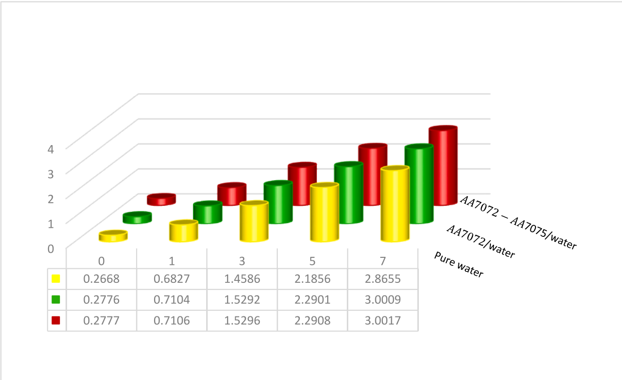

(b)

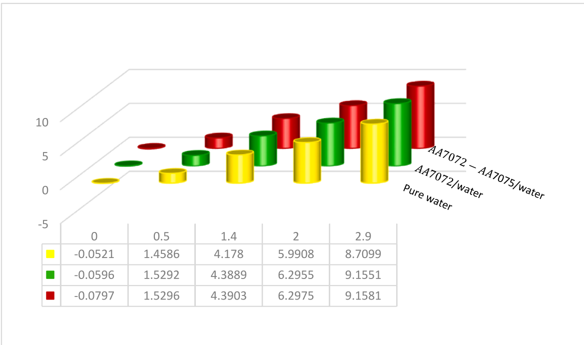

(c)

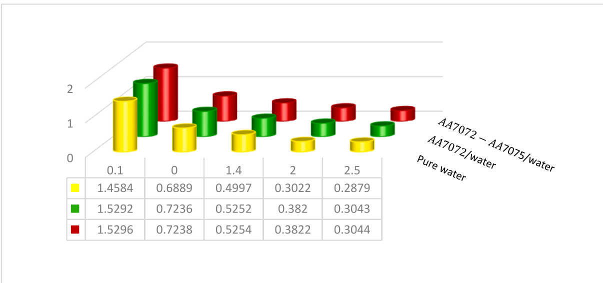

(d)

Fig. 8. Nusselt number for various values of (a) Suction (S), (b) Magnetic Constrains (M), (c) Eckert number (Ec), and (d) Thermal slip (γ).

Table 3
Effects of governing parameters on wall temperature $T(0)$ for pure water, AA7072/water, and AA7075-AA7072/water.

M	S	Ec	γ	Pure water	AA7072/water	AA7075-AA7072/water
0	1	0.5	0.1	1.02668	1.02695	1.02695
1				1.6789	1.06900	1.06901
3				1.14600	1.14861	1.14864
5				1.21889	1.22268	1.22272
7				1.28713	1.29194	1.29200
3	0.5			1.16398	1.16564	1.16567
	1.5			1.11223	1.11503	1.11507
	2.0			1.08678	1.08925	1.08928
	2.3			1.07548	1.07772	1.07775
	1	0		0.99478	0.99420	0.99420
		1.4		1.41820	1.42653	1.42662
		2.0		1.59965	1.61182	1.61195
		2.9		1.87183	1.88972	1.88992
		0.5	0.9	1.62103	1.63330	1.63344
			1.4	1.70044	1.71542	1.71560
			2.0	1.72638	1.74381	1.74401
			2.5	1.72203	1.74110	1.74132

- Eckert number increases the temperature, Nusselt number, and wall temperature.
- Thermal slip effect reduces the temperature from the system and for wall temperature.
- Shrinking sheet movement plays a key role in manipulating fluidity and thermal dispersal.
- Hybridity combination of flow fluid stays ahead of the other two traditional fluids such as pure water and nanofluid to explore such studies.

6Future scope

This work can be extended in the future with different hybrid combinations of flow fluids. Entropy and CFD analysis can be performed with vital fluid combinations. Shape, stretching side, and physical aspects around the sheet will provide us the numerous future scopes. The Crank-Nicolson method could be applied to a variety of physical and technical challenges in the future [49–61].

Credit author statement

- Conceptualization: Rabha W. Ibrahim,
- Formal analysis: Suriya Uma Devi. S,
- Investigation: Mohamed R. Eid.
- Methodology: Wasim Jamshed.
- Software: Hanifa Hanif.
- Writing - original draft: Mohamed R. Eid & Sharidan Shafie.
- Writing - review editing: Aeshah A. Raezah & Sayed M El Din.
- Numerical process breakdown: Wasim Jamshed & Aeshah A. Raezah.
- Re-modelling design: Aeshah A. Raezah.
- Re-validation: Sayed M El Din.

Declaration of competing interest

The authors declare that they have no known competing financial interests or personal relationships that could have appeared to influence the work reported in this paper.

Data availability

Data will be made available on request.

Acknowledgements

The authors extend their appreciation to the Deanship of Scientific Research at King Khalid University, Abha, Saudi Arabia, for funding this work through the Research Group Project under Grant Number (RGP.2/154/43).

Appendix A. Supplementary data

Supplementary data to this article can be found online at https://doi.org/10.1016/j.csite.2023.102707.

References

[1] Mustafa Turkyilmazoglu, Single phase nanofluids in fluid mechanics and their hydrodynamic linear stability analysis, Comput. Methods Progr. Biomed. 187 (2020), 105171.

[2] Hanifa Hanif, A finite difference method to analyze heat and mass transfer in kerosene based γ-oxide nanofluid for cooling applications, Phys. Scripta 96 (9) (2021), 095215.

[3] Zafar Said, L. Syam Sundar, Arun Kumar Tiwari, Hafiz Muhammad Ali, Mohsen Sheikholeslami, Evangelos Bellos, Hamza Babar, Recent advances on the fundamental physical phenomena behind stability, dynamic motion, thermophysical properties, heat transport, applications, and challenges of nanofluids, Phys. Rep.946 (2021) 1–94.

[4] Dipak Kumar Mandal, Nirmalendu Biswas, K. Nirmal, Manna, Dilip Kumar Gayen, Rama Subba Reddy Gorla, Ali J. Chamkha, Thermo-fluidic transport process in a novel M-shaped cavity packed with non-Darcian porous medium and hybrid nanofluid: application of artificial neural network (ANN), Phys. Fluids 34 (3) (2022), 033608.

[5] Abhinav Saha, Nirmal K. Manna, Koushik Ghosh, Nirmalendu Biswas, Analysis of geometrical shape impact on thermal management of practical fluids using square and circular cavities, Eur. Phys. J. Spec. Top. (2022) 1–29.

[6] Kadhim K. Al-Chlaihawi, Hussein H. Alaydamee, Ahmed E. Faisal, Khaled Al-Farhany, and Mohammed A. Alomari. "Newtonian and non-Newtonian nanofluids with entropy generation in conjugate natural convection of hybrid nanofluid-porous enclosures: a review, Heat Transfer 51 (2) (2022) 1725–1745.

[7] Maisarah Kursus, Pay Jun Liew, Nor Azwadi Che Sidik, Jingsi Wang, Recent progress on the application of nanofluids and hybrid nanofluids in machining: a comprehensive review, Int. J. Adv. Manuf. Technol. (2022) 1–27.

[8] Tahar Tayebi, Analysis of the local non-equilibria on the heat transfer and entropy generation during thermal natural convection in a non-Darcy porous medium, Int. Commun. Heat Mass Tran. 135 (2022), 106133.

[9] Tahar Tayebi, Ali J. Chamkha, Hakan F. Öztop, Lynda Bouzeroura, Local thermal non-equilibrium (LTNE) effects on thermal-free convection in a nanofluid-saturated horizontal elliptical non-Darcian porous annulus, Math. Comput. Simulat. 194 (2022) 124–140.

[10] Qingang Xiong, Sam Altnji, Tahar Tayebi, Mohsen Izadi, Hajjar Ahmad, Bengt Sundén, Larry KB. Li, A comprehensive review on the application of hybrid nanofluids in solar energy collectors, Sustain. Energy Technol. Assessments 47 (2021), 101341.

[11] M. Muneeshwaran, G. Srinivasan, P. Muthukumar, Chi-Chuan Wang, Role of hybrid-nanofluid in heat transfer enhancement–A review, Int. Commun. Heat Mass Tran. 125 (2021), 105341.

[12] Vineet Dubey, Anuj Kumar Sharma, A short review on hybrid nanofluids in machining processes, Adv. Mater. Process. Technol. (2022) 1–14.

[13] Syed M. Hussain, Wasim Jamshed, A comparative entropy based analysis of tangent hyperbolic hybrid nanofluid flow: implementing finite difference method, Int. Commun. Heat Mass Tran. 129 (2021), 105671.

[14] Hanifa Hanif, Sharidan Shafie, Rozaini Roslan, Anati Ali, Collision of Hybrid Nanomaterials in an Upper-Convected Maxwell Nanofluid: a Theoretical Approach, Journal of King Saud University - Science, 2022, 102389.

[15] Wasim Jamshed, M. Prakash, S. Devi, Rabha W. Ibrahim, Faisal Shahzad, Kottakkaran Sooppy Nisar, Mohamed R. Eid, Abdel-Haleem Abdel-Aty, M. Motawi Khashan, I.S. Yahia, A brief comparative examination of tangent hyperbolic hybrid nanofluid through a extending surface: numerical Keller–Box scheme, Sci. Rep. 11 (1) (2021) 1–32.

[16] Hanifa Hanif, Sharidan Shafie, Interaction of multi-walled carbon nanotubes in mineral oil based Maxwell nanofluid, Sci. Rep. 12 (1) (2022) 1–16.

[17] Lijun Zhang, M.M. Bhatti, Efstathios E. Michaelides, M. Marin, R. Ellahi, Hybrid nanofluid flow towards an elastic surface with tantalum and nickel nanoparticles, under the influence of an induced magnetic field, Eur. Phys. J. Spec. Top. 231 (3) (2022) 521–533.

[18] Hanifa Hanif, Ilyas Khan, Sharidan Shafie, A novel study on time-dependent viscosity model of magneto-hybrid nanofluid flow over a permeable cone: applications in material engineering, Euro Phys. J. Plus. 135 (9) (2020) 730.

[19] Hanifa Hanif, Ilyas Khan, Sharidan Shafie, A novel study on hybrid model of radiative Cu–Fe_3O_4/water nanofluid over a cone with PHF/PWT, Eur. Phys. J. Spec. Top. 230 (5) (2021) 1257–1271.

[20] Abed Mourad, Abderrahmane Aissa, Fateh Mebarek-Oudina, Wasim Jamshed, Waleed Ahmed, Hafiz Muhammad Ali, A.M. Rashad, Galerkin finite element analysis of thermal aspects of Fe_3O_4-MWCNT/water hybrid nanofluid filled in wavy enclosure with uniform magnetic field effect, Int. Commun. Heat Mass Tran. 126 (2021), 105461.

[21] Nirmal K. Manna, Milan K. Mondal, Nirmalendu Biswas, A novel multi-banding application of magnetic field to convective transport system filled with porous medium and hybrid nanofluid, Phys. Scripta 96 (6) (2021), 065001.

[22] Najiyah Safwa Khashi'ie, Iskandar Waini, Norihan Md Arifin, Ioan Pop, Unsteady squeezing flow of Cu-Al_2O_3/water hybrid nanofluid in a horizontal channel with magnetic field, Sci. Rep. 11 (1) (2021) 1–11.

[23] Muhammad Saqib, Hanifa Hanif, T. Abdeljawad, Ilyas Khan, Sharidan Shafie, K. Sooppy Nisar, Heat transfer in MHD flow of maxwell fluid via fractional Cattaneo-Friedrich model: a finite difference approach, Comput. Mater. Continua (CMC) 65 (3) (2020) 1959–1973.

[24] Hanifa Hanif, Sharidan Shafie, Noraihan Afiqah Rawi, Abdul Rahman Mohd Kasim, Entropy analysis of magnetized ferrofluid over a vertical flat surface with variable heating, Alex. Eng. J. 65 (15) (2022) 897–908.

[25] Hamzeh Alkasasbeh, Numerical solution of heat transfer flow of casson hybrid nanofluid over vertical stretching sheet with magnetic field effect, CFD Lett. 14 (3) (2022) 39–52.

[26] Nepal Chandra Roy, Anwar Hossain, Ioan Pop, Flow and heat transfer of MHD dusty hybrid nanofluids over a shrinking sheet, Chin. J. Phys. 77 (2022) 1342–1356.

[27] Mehdi Khazayinejad, S.S. Nourazar, Space-fractional heat transfer analysis of hybrid nanofluid along a permeable plate considering inclined magnetic field, Sci. Rep. 12 (1) (2022) 1–15.

[28] Mehmet Gürdal, Hayati Kadir Pazarlıoğlu, Mutlu Tekir, Fethi Murat Altunay, Kamil Arslan, Engin Gedik, Implementation of hybrid nanofluid flowing in dimpled tube subjected to magnetic field, Int. Commun. Heat Mass Tran. 134 (2022), 106032.

[29] N.S. Khashi'ie, N.M. Arifin, I. Pop, N.S. Wahid, Flow and heat transfer of hybrid nanofluid over a permeable shrinking cylinder with Joule heating: a comparative analysis, Alex. Eng. J. 59 (3) (2020) 1787–1798.

[30] M. Shoaib, M.A.Z. Raja, M.T. Sabir, M. Awais, S. Islam, Z. Shah, P. Kumam, Numerical analysis of 3-D MHD hybrid nanofluid over a rotational disk in presence of thermal radiation with Joule heating and viscous dissipation effects using Lobatto IIIA technique, Alex. Eng. J. 60 (4) (2021) 3605–3619.

[31] Hanifa Hanif, Sharidan Shafie, Impact of Al2O3 in electrically conducting mineral oil-based maxwell nanofluid: application to the petroleum industry, Fract. Fraction. 6 (4) (2022) 180.

[32] Hanifa Hanif, Sharidan Shafie, Application of Cattaneo heat flux to Maxwell hybrid nanofluid model: a numerical approach, Euro Phys. J. Plus. 137 (8) (2022) 1–13.

[33] I. Waini, A. Ishak, I. Pop, Radiative and magnetohydrodynamic micropolar hybrid nanofluid flow over a shrinking sheet with Joule heating and viscous dissipation effects, Neural Comput. Appl. 34 (5) (2022) 3783–3794.

[34] N.A. Zainal, R. Nazar, K. Naganthran, I. Pop, Magnetic impact on the unsteady separated stagnation-point flow of hybrid nanofluid with viscous dissipation and Joule heating, Mathematics 10 (13) (2022) 2356.

[35] S. Hussain, T. Tayebi, T. Armaghani, et al., Conjugate natural convection of non-Newtonian hybrid nanofluid in wavy-shaped enclosure, Apl. Math. Mech. Engl. Ed. 43 (2022) 447–466.

[36] Tahar Tayebi, Ali J. Chamkha, Ammar A. Melaibari, Elhadj Raouache, Effect of internal heat generation or absorption on conjugate thermal-free convection of a suspension of hybrid nanofluid in a partitioned circular annulus, Int. Commun. Heat Mass Tran. 126 (2021), 105397.

[37] A. Sattar Dogonchi, Tahar Tayebi, Nader Karimi, Ali J. Chamkha, Hesham Alhumade, Thermal-natural convection and entropy production behavior of hybrid nanoliquid flow under the effects of magnetic field through a porous wavy cavity embodies three circular cylinders, J. Taiwan Inst. Chem. Eng. 124 (2021) 162–173.

[38] T. Tayebi, A.J. Chamkha, Effects of various configurations of an inserted corrugated conductive cylinder on MHD natural convection in a hybrid nanofluid-filled square domain, J. Thermal Anal. Calorimetry. (2021) 1399–1411.
[39] Tahar Tayebi, Hakan F. Öztop, Ali J. Chamkha, Natural convection and entropy production in hybrid nanofluid filled-annular elliptical cavity with internal heat generation or absorption, Therm. Sci. Eng. Prog. 19 (2020), 100605.
[40] C. Venance, M.N. Kinyanjui, K.e. Giterere, Effects of thermo-conductivity on hydromagnetic nanofluid convective flow through an artificial kidney past a porous stretching cylinder, Math. Probl Eng. 2022 (2022), 5468057.
[41] H. Hanif, S. Shafie, Impact of Al_2O_3 in electrically conducting mineral oil-based maxwell nanofluid: application to the petroleum industry, Fract. Fraction. 6 (4) (2022) 180.
[42] A. Hiremath, G.J. Reddy, H. Basha, N. Narayanan, O. Anwar Bég, Magnetized supercritical third-grade nanofluid flow from a vertical cylinder using a Crank–Nicolson implicit scheme, Waves Random Complex Media (2022) 1–32.
[43] Hanifa Hanif, Cattaneo–Friedrich and Crank–Nicolson analysis of upper-convected Maxwell fluid along a vertical plate, Chaos, Solit. Fractals 153 (2021), 111463.
[44] Hanifa Hanif, Cattaneo–Friedrich and Crank–Nicolson analysis of upper-convected Maxwell fluid along a vertical plate, Chaos, Solit. Fractals 153 (2021), 111463.
[45] A. Hiremath, A, G.J. Reddy, O.A. Bég, H. Holla, Numerical investigation on transient third-grade magnetized nanofluid flow and radiative convection heat transfer from a stationary/moving cylinder: nanomaterial and nanoparticle shape effects, Waves Random Complex Media (2022) 1–30.
[46] Muhammad Sajjad, Mujtaba Ali, Adnan Asghar, Teh Yuan Ying, Dual solutions of magnetohydrodynamics Al_2O_3+Cu hybrid nanofluid over a vertical exponentially shrinking sheet by presences of Joule heating and thermal slip condition, CFD Lett 14 (8) (2022) 100–115.
[47] Hanifa Hanif, Ilyas Khan, Sharidan Shafie, Heat transfer exaggeration and entropy analysis in magneto-hybrid nanofluid flow over a vertical cone: a numerical study, J. Therm. Anal. Calorim. 141 (5) (2020) 2001–2017.
[48] Ullah Adnan, S.I. Khan, U. Khan, et al., Thermal transport investigation in AA7072 and AA7075 aluminum alloys nanomaterials based radiative nanofluids by considering the multiple physical flow conditions, Sci. Rep. 11 (2021) 9837.
[49] Ammar I. Alsabery, Tahar Tayebi, Ali J. Chamkha, Ishak Hashim, Natural convection of Al_2O_3-water nanofluid in a non-Darcian wavy porous cavity under the local thermal non-equilibrium condition, Sci. Rep. 10 (2020), 18048.
[50] Ammar I. 1 Alsabery, Tahar 2 Tayebi, Ali J. 3 Chamkha, Ishak Hashim, Effects of two-phase nanofluid model on natural convection in a square cavity in the presence of an adiabatic inner block and magnetic field, Int. J. Numer. Methods Heat Fluid Flow 28 (7) (2018) 1613–1647, 35.
[51] W. Jamshed, A. Aziz, Cattaneo–Christov based study of TiO2–CuO/EG Casson hybrid nanofluid flow over a stretching surface with entropy generation, Appl. Nanosci. 8 (2018) 685–698.
[52] W. Jamshed, Numerical investigation of MHD impact on maxwell nanofluid, Int. Commun. Heat Mass Tran. 120 (5) (2021) 683.
[53] W. Jamshed, K.S. Nisar, Computational single phase comparative study of Williamson nanofluid in parabolic trough solar collector via Keller box method, Int. J. Energy Res. 45 (7) (2021) 10696–10718.
[54] W. Jamshed, K.S. Nisar b, R.W. Ibrahim, F. Shahzad, M.R. Eid, Thermal expansion optimization in solar aircraft using tangent hyperbolic hybrid nanofluid: a solar thermal application, J. Mater. Res. Technol. 14 (2021) 985–1006.
[55] W. Jamshed, Finite element method in thermal characterization and streamline flow analysis of electromagnetic silver-magnesium oxide nanofluid inside grooved enclosure, Int. Commun. Heat Mass Tran. 130 (2021), 105795.
[56] W. Jamshed, M.R. Eid, A.F. Al-Hossainy, Z. Raizah, E.S.M. Tag El Din, T. Sajid, Experimental and TDDFT materials simulation of thermal characteristics and entropy optimized of Williamson Cu-methanol and Al_2O_3-methanol nanofluid flowing through solar collector, Sci. Rep. 12 (2022), 18130.
[57] N. Islam, A.A. Pasha, W. Jamshed, R.W. Ibrahim, R. Alsulami, On Powell-Eyring hybridity nanofluidic flow based Carboxy-Methyl-Cellulose (CMC) with solar thermal radiation: a quadratic regression estimation, Int. Commun. Heat Mass Tran. 138 (2022), 106413.
[58] A.A. Pasha, N. Islam, W. Jamshed, M.I. Alam, A.G.A. Jameel, K.A. Juhany, R. Alsulami, Statistical analysis of viscous hybridized nanofluid flowing via Galerkin finite element technique, Int. Commun. Heat Mass Tran. 137 (2022), 106244.
[59] G. Rasool, A. Shafiq, S. Hussain, M. Zaydan, A. Wakif, A.J. Chamkha, M.S. Bhutta, Significance of rosseland's radiative process on reactive maxwell nanofluid flows over an isothermally heated stretching sheet in the presence of Darcy–forchheimer and Lorentz forces: towards a new perspective on buongiorno's model, Micromachines 13 (2022) 368, https://doi.org/10.3390/mi13030368.
[60] G. Rasool, A.M. Saeed, A.I. Lare, A. Abderrahmane, K. Guedri, H. Vaidya, R. Marzouki, Darcy-forchheimer flow of water conveying multi-walled carbon nanoparticles through a vertical cleveland Z-staggered cavity subject to entropy generation, Micromachines 13 (2022) 744, https://doi.org/10.3390/mi13050744.
[61] Ghulam Rasool, Nehad Ali Shah, R. Essam, El-Zahar, Abderrahim Wakif, Numerical investigation of EMHD nanofluid flows over a convectively heated riga pattern positioned horizontally in a Darcy-Forchheimer porous medium: application of passive control strategy and generalized transfer laws, Waves Random Complex Media (2022), https://doi.org/10.1080/17455030.2022.2074571.